ELSEVIER

Ceramics International 31 (2005) 333–347

CERAMICS INTERNATIONAL

www.elsevier.com/locate/ceramint

Influence of gel-derived nanocrystalline spinel in a high alumina castable: Part 1

S. Ghosh, T. Maiti, S. Sen, S. Mukhopadhyay*

College of Ceramic Technology, 73, A.C. Banerjee Lane, Kolkata 700010, India

Received 24 March 2004; received in revised form 26 April 2004; accepted 8 June 2004
Available online 25 September 2004

Abstract

A newer class of spinel-alumina castable was fabricated by incorporating 8.0 wt.% of modified spinel additives synthesized via sol–gel and coprecipitation methods. These additives prepared by cheaper ingredients after optimum grinding and calcination, were characterized in terms of particle size distribution, infrared spectra and X-ray diffraction patterns. The properties of those spinel-alumina castables, with another prepared by the same amount of commercial preformed spinel fine, were studied and compared. Cold crushing strength, apparent porosity, hot modulus of rupture, pore size distribution, scanning electron microscopy, energy dispersive spectral analysis, thermal shock and slag corrosion resistance tests of selected samples were done to identify the immense prospect of sol–gel additive. Transmission electron microscope (with SAED facility) was also utilized to establish the nanocrystalline feature of the sol–gel additive.

Keywords: A. Sol–gel process; B. Microstructure; C. Thermal shock resistance; D. Spinel; Castable

1. Introduction

Steel being a very much important and extensively used engineering material with an amazing range of properties, requires special attention for its production and refining [1]. The final cleaning of steel as desired by the end-user, is accomplished by secondary refining in the ladle. In this method, the partly refined steel tapped from steel-making furnace is taken into ladle and refined by any one or a combination of ladle metallurgical processes [2,3]. These secondary refining processes extend the period of contact of superheated steel with the ladle refractory materials in a severely corrosive atmosphere. In the modern ladles, the improved performance of high alumina based refractory castables in lieu of shaped alumina bricks has been well established [4]. These unshaped castables in various forms (e.g. low, ultralow and no cement, etc.) are, however, becoming increasingly popular in both ferrous and non-ferrous industries due to a number of operational flexibilities they possess compared to the shaped refractories [5–7]. Recently spinel-alumina castables are being abundantly used in ladle lining, continuous casting and electric arc furnaces [8–11] to exploit the superb qualities of magnesium aluminate spinel. Among these properties, its chemical nature has been given a special importance which exhibits remote subtlety with tetrahedral and octahedral voids located inside cubic crystalline structure [12,13]. Preformed or prereacted commercial spinels are widely used for preparing spinel-alumina monolithic castables. However, such spinels are expensive due to extremely high sintering temperature (nearly, 1900 °C) associated with some careful and lengthy steps of production, namely, precalcination, co-grinding, drying, granulating and so on [14–16]. Another common practice to prepare the same type castable is with in situ or self-forming spinels where fine magnesia powder taken in the batch reacts with alumina fines present in castable matrix to result in spinel [17,18] at service temperature. However, this process is associated with excessive volume expansion, dusting and hydration problem during fabrication with the appearance of dawsonite and hydrotalcite phases [19–21]. Some recent publications proposed another method of fabrication of in situ spinel-

E-mail address: msunanda_cct@yahoo.co.in (S. Mukhopadhyay).

0272-8842/$30.00
doi:10.1016/j.ceramint.2004.06.001

alumina castables by utilizing hydrated spinel precursors in the castable batch [22–30]. Such nano and microfine precursors were synthesized in laboratory by cost effective chemicals, respectively, via sol–gel and coprecipitation routes [22,31–37]. The castables bonded with sol–gel precursor, showed better homogeneity and spalling resistance with a scope of temperature and time saving than required for preformed spinel-alumina castables. However, such in situ type castables conspicuously showed the pitfalls originated by volume stress and release of excessive fugitives from precursor gels. More importantly, the solid content of those precursors being very low [24,26–28], it was difficult to incorporate them in batch in larger quantity without a tremendous sacrifice in green strength and installation flexibility [38].

Recently the nanostructured materials are being utilized and investigated by a broad spectrum of researchers from several disciplines [39]. These materials also secured their entry and application in the field of refractories [40,41]. The effect of nanofine sol–gel-derived hydrated spinel precursor in castable has been reported in our previous papers [22–24,26]. The present investigation attempts to formulate and evaluate a newer and modified version of in situ spinel-alumina castables fabricated by optimally ground and calcined form of those gel precursors. The advantage of retention of nanocrystallinity of the sol–gel type spinel additive has been discussed here by making a comparative analysis of the performance of three kinds of spinel-alumina castables. In this regard, the shortfall of the earlier work has also been emphasized briefly to clarify the improvement achieved in this later stage.

2. Experimental

The formulation of original spinel-free castable (Table 1) was estimated by the optimum packing efficiency calculated from the distribution modulus (q-value) of the composition [7,42–43]. In this respect, the particle size distribution and amount of different constituents, e.g. white fused alumina ($-6+16$, $-16+30$, $-30+60$, -100 mesh BS) and other finer fractions, were given special consideration. The characteristics of different hydrated $MgAl_2O_4$ precursors applied to castable in different concentrations, namely the sol–gel (G type) and the coprecipitated gel (C type), have been shown in Table 2(a). These in situ spinel precursors were prepared in laboratory from cheaper ingredients that had been discussed in detail in our previous article [24], together with the categorical determination of their special characteristics as shown in Table 2(a). The concentration (wt.%) of these precursors added to the castable batch (Table 1) was increased twice in each five successive stages (0.25, 0.5, 1.0, 2.0 and 4.0 wt.%) and the effects were studied. It has been observed that the last slab (4.0 wt.%) was detrimental as regards green strength and installation flexibility of castable [26,27,38]. As such the concentration of precursors in castable was not increased beyond 4.0 wt.%. It has also been reported [44] that this gel mass is effective in small quantity when added to a bulk ceramic body. These hydrated spinel-bonded high alumina-based monoliths were cast in cube (25.4 mm) and bar (150 mm × 25 mm × 25 mm) type moulds, gently tapped by hands with no extra mechanical vibration needed from outside. They were allowed to set in different types of humid atmospheres, for at least 24 h in each. After getting them released from moulds, these were dried in open atmosphere (25 °C) for one day and then in oven (110 °C) for three days at a stretch. Finally the castables (also named as C and G types according to the precursors applied to them) were fired at elevated temperatures, e.g. 900, 1200 and 1500 °C with a soaking for 2 h in each case.

In the second and main part of the work, a newer version of in situ spinel was prepared [Table 2(b)]. In this respect, the semidried gel precursors (G and C) were ground in agate mortar with pestle for 1 h [45,46]. They were optimally calcined [47] to 900 °C (with 2 h soaking) and finally ground again by agate for 1 h [36], without any expensive instrument like vibrogrinder or ball mill. A fineness below

Table 1
Batch composition of original spinel-free castable

Constituents	Amount (wt.%)
Aggregate (white fused alumina:coarse medium and fine)	77
Matrix (microsilica, micronized alumina, refractory cement)	23
Total	100
Deflocculant (%)	0.05
Water (%)	5–6

Table 2
Characteristics of two types of (a) hydrated in situ spinel precursors incorporated to the castable batch shown in Table 1 and (b) modified in situ spinel additives (powdery) incorporated to the new castable batch shown in Table 3

(a)

Characteristics	Coppt. spinel (C)	Sol–gel spinel (G)
Solid content (%)	~10.0	~10.0
pH	6–7	3–4
Average particle size	6 μm	11 nm
Surface area (m^2/gm)	22	178

(b)

Characteristics	Sol–gel-derived	Coprecipitated
Particle size (μm)	Below 75	Below 75
Crystal phases fully appeared at (°C)	600	1000
Respective crystallite size (apparent)	18 nm	0.14 μm
Al_2O_3 (wt.%)	71.5	73.3
MgO (wt.%)	28.5	26.7
True specific gravity	3.02	2.46

Table 3
Formulation of new castable batch including spinel as preformed or modified in situ powder

Constituents	Amount (wt.%)
Aggregate (white fused alumina: coarse, medium, fine)	75
Microsilica	1
Refractory cement	6
Micronized alumina	10
Spinel fine [either preformed (P) or modified in situ (G or C); one at a time]	8
Total (q-value = 0.2; water, 6.0 %)	100

75 μm was achieved after sieving them through 200 mesh (BS) and these powders were termed as modified in situ spinel additives. As reported in literature [17,48], fine powders below 75 μm size may be considered as the matrix constituent in a castable batch. Accordingly, a new castable batch (Table 3) was formulated in this second stage of investigation. A commercial preformed spinel powder (P), known to be rich in alumina was collected from the market and characterized (Table 4) as reported before [27,29]. All these three kinds of powders (G, C and P) were utilized one at a time in that new castable batch (Table 3) separately in the same amount (8.0 wt.%). These newer spinel-alumina castables were coded, respectively, as GN, CN and PN types. All of them were fabricated by the same procedure discussed in the last paragraph and fired up to 1600 °C without any deformation of the bulk materials. It should be mentioned that as the microsilica content of the previous batch (Table 1) was too high (5.0 wt.%), the samples showed noticeable distortion at 1600 °C possibly due to the generation of low melting phases [49–51]. Microsilica content in the new batch was reduced to 1.0% (Table 3) to keep the provision open in future study to compare the properties of castables by replacing spinel fines with magnesia powder, where very little microsilica is conventionally added [17,18,50]. The raw materials used in Table 3 were the same as used in Table 1; their chemical analyses had been shown in our previous articles [24,26]. The amount of each ingredient (Table 3) was adjusted to retain good packing and self-flow criteria [7,42,43] of this new batch with a q-value around 0.2.

The particle size distribution of the modified additive was studied in Mastersizer E.Ver.1.2b model. The transmission electron micrograph and selective area electron diffraction (SAED) patterns were taken by the instrument Hitachi H-600 bright field electron microscope with an accelerating voltage of 50 kV. The IR (infra red) spectroscopy study of spinel additives were performed with an instrument 'Perkin-Elmer' (model) by KBr method. Apparent porosity (AP) and cold crushing strength (CCS) of the three types of castables were done by standard methods [52]. The hot modulus of rupture (HMOR) test of some selected samples was obtained by an instrument, make Naskar & Co. (India) at 1400 °C having a microprocessor controlled loading system with a rate 1.27 kg/s; it was basically a three-point bending method done with the fired castable bars. An average result of four samples was taken for all these tests. The thermal shock resistance of prefired castables (1500 °C) was estimated in terms of percent residual strength (%RS), which is the CCS value retained by the samples after five cycles of thermal shock; each cycle included heating the samples at 800 °C for 10 min followed by quenching them in water at room temperature for another 10 min. The pore size distribution patterns of fired GN and PN type castables were taken from Mercury Porosimeter Instrument (model Poremaster-33, Quantachrome Version 4.01). The additives and castables were subjected to XRD phase analysis by using Ni filtered CuKα at 40 kV/20 mA. For microstructural studies, SEM (with EDS) experiment was conducted with the help of the instruments JEOL JSM 5200 and Hitachi S-2300 models. To determine the slag corrosion resistance, a cylindrical groove was made at the middle of some castable cubes at green stage and these were preheated to 1200 °C for 2 h. The grooves were filled up with converter slag supplied from VSL, India (Table 5) and fired at 1500 °C. After normal cooling, the withered samples were examined to correlate the susceptibility of modified spinel additive in aggressive condition of steel refining.

Table 4
Characteristics of preformed magnesium aluminate fines

Characteristics	P type spinel
Major constituents (wt.%)	
Al_2O_3	>77.0
MgO	>22.0
True specific gravity	3.58
Particle size (μm)	Below 45

Table 5
Composition of converter slag

Constituents	Content (wt.%)
CaO	47.6
SiO_2	15.0
MgO	10.6
FeO	20.5
Al_2O_3	1.3
MnO	2.0
Basicity	More than 3.0

3. Results and discussion

Fig. 1(a) shows the ordinary photograph of hydrated spinel gel (G), transparent and amorphous in nature. It has been reported [24] that the sol–gel precursor contains nanofine particles while that of the coprecipitate is in micron ranges [Table 2(a)]. The high specific surface area of G precursor in comparison to the agglomerated C precursor is a real advantage that has been exploited to prepare in situ spinel-alumina castables. It has been shown [26,29] that the thermal shock resistance of G-bonded castable was even

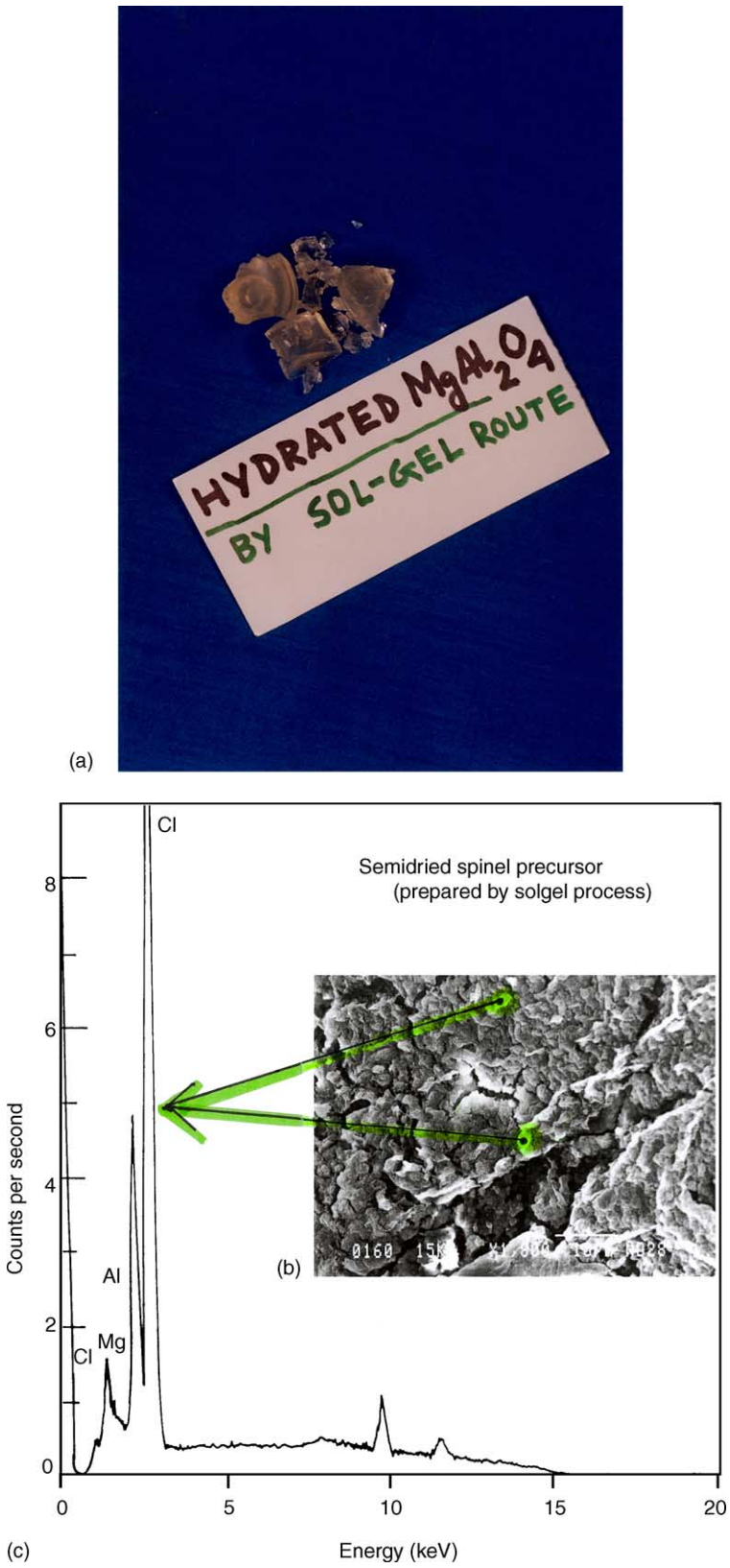

Fig. 1. (a) Photograph of hydrated $MgAl_2O_4$ (G) precursor prepared by sol–gel method; (b) SEM of dried gel relict (G) and (c) EDS trace taken at a specific microrelict.

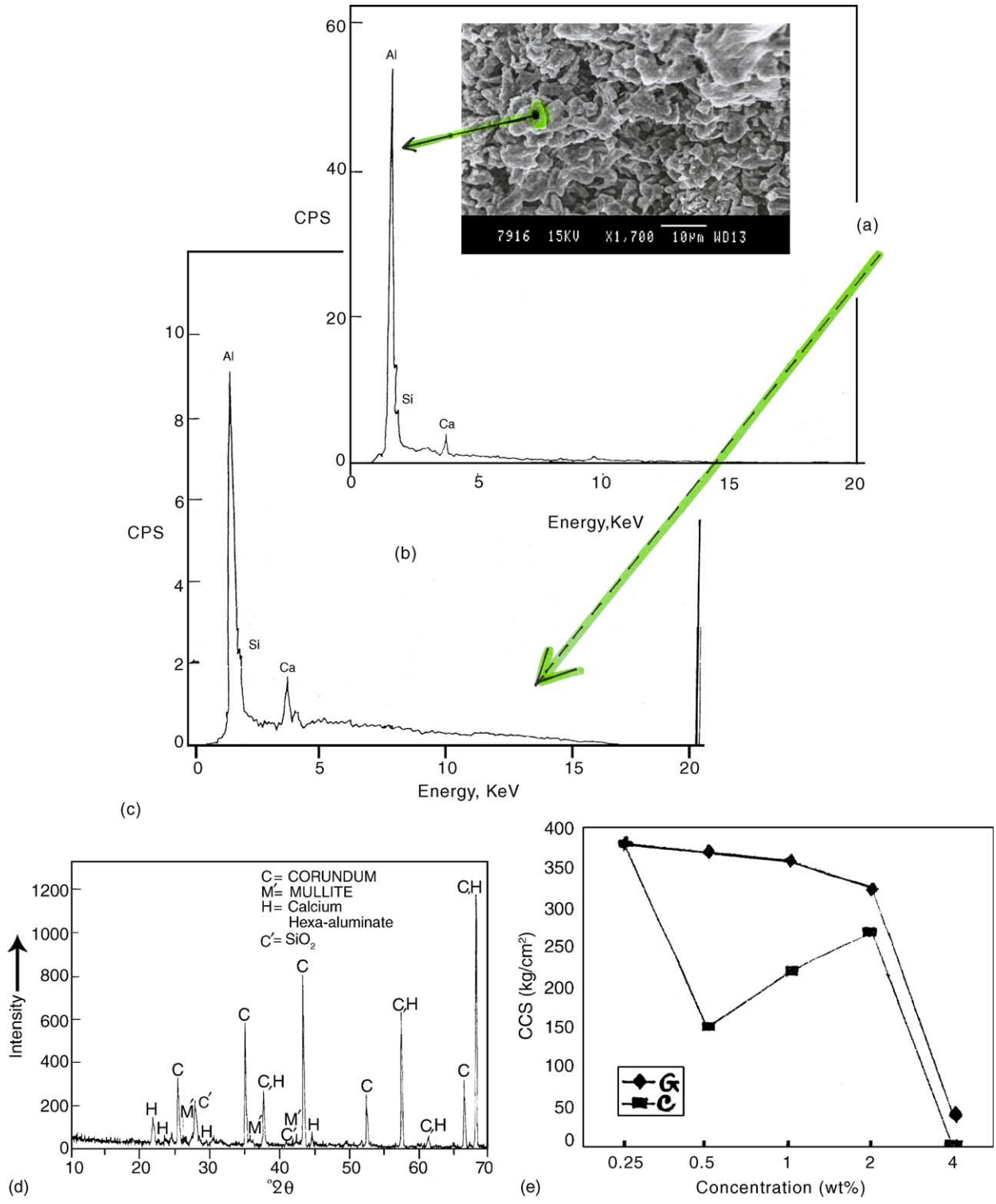

Fig. 2. (a) Micrograph of the fired matrix part (1500 °C/2 h) of original spinel-free castable; (b) EDS pattern at a specific point in the matrix; (c) EDS pattern of average composition of the whole matrix; (d) XRD pattern of the fired matrix part (1500 °C/2 h) of original spinel-free castable and (e) comparison of green strength (110 °C/2 h) of castables bonded with increasing concentration (0.25–4.0 wt.%) of sol–gel and coprecipitate precursors.

much improved than preformed spinel-alumina castable. It was suggested that the tuning of pore sizes and their distribution achieved from the pliant sol–gel precursor might upgrade the spalling resistance [53]. On the contrary, the agglomerated C precursor with the same solid content [Table 2(a)] failed to exhibit such crack-arresting behaviour possibly due to generation of uncontrolled larger pores and cracks created in castable which themselves behaved as major flaws and enhanced the heterogeneity of the system. Fig. 1(b) and (c) show the SEM and EDS of the dried gel

relict (G). The continuous crack in the gel might have appeared due to the capillary stress generated during shrinkage and removal of entrapped water. The microrelicts generated throughout the bulk gel are very prominent which contain a significant amount of chlorine coming from the starting material [22]. Each microrelict, as confirmed from EDS, shows a close (1:1) composition of Mg and Al observed in $MgAl_2O_4$. It is suggested that these tiny domains of gel, in due course of heating, retain their precision in composition in the modified spinel powder as corroborated later. The beauty of this sol–gel route is the atomic scale mixing of the ingredients unlike the coprecipitation method. The latter yields uncontrolled aggregated particles by coarser scale mixing of ingredients which deviates from the spinel stoichiometry upon further heating [Table 2(b)]. The additional benefits of the spinel from sol–gel precursor are its contributions in castables as regards better slag corrosion resistance and physical properties [24]. Although their solid content is very low [Table 2(a)], still these nanofine precursors show better performance seemingly due to high surface to volume ratio and greater yield strength of nanoparticles. The advantage of significantly less amount of nanofine particles in ceramic materials has been already touched upon by several researchers [54], which ensure reliability, strength, thermal shock and corrosion resistances. However, the previous stage of our work involving these G and C precursors left some rooms open for further development.

Firstly, the original spinel-free batch of castable [code B, Table 1] showed very poor hot strength of 65 kg/cm^2. Its good packing efficiency, q-value and physical properties have been described before [24] together with its disadvantage (with less HMOR) originated by excess (5.0 wt.%) microsilica in batch. Such inherent flaw of the initial batch (Table 1) is further confirmed by Fig. 2(a)–(c). Fig. 2(a) is the micrograph of the fired matrix part of that castable which shows well homogeneity and connectivity of the constituents. Although mullite phase existing in that matrix is confirmed by XRD [Fig. 2(d)] and EDS at a specific point [Fig. 2(b)], yet the whole region of the figure was enriched with lime. This is evident from the EDS of the overall composition [Fig. 2(c)] and as such that low melting C–A–S ($CaO–Al_2O_3–SiO_2$) phase adversely affected the hot property of that castable [Table 6].

The second pitfall of the earlier work included the characteristics of hydrated G and C precursors. Spinel-forming reaction itself is known to be volume expansive [12,19] and was further triggered by these chemically prepared gels. As such the castables bonded with them contained too much flaws as compared to the same bonded by preformed spinel additives. Their solid content being only 10.0 wt.%, enormous porosity was introduced in the respective castables. These pores, if not tuned as regards their size and distribution, must impart a severe detriment to slag corrosion and mechanical properties as manifested with C bonded castables. More importantly, when the amount of these precursors was successively increased in castable, viz. 0.25, 0.5, 1.0, 2.0 and 4.0 wt.%, the last slab revealed a miserable failure of green strength and installation capability. This is confirmed from Fig. 2(e), showing very poor green strength of castables bonded with 4.0 wt.% of G and C precursors. Basically, the net solid coming from them was 0.4% and the rest part was water, which created this practical inconvenience. For this reason we had to fix the concentration of gel precursor between 0.5 and 2.0 wt.% in castables as reported earlier [24,26–29]. The first slab (i.e. 0.25%) with only 0.025% of solid had not remarkably influenced the properties of original (Table 1) castable. The second slab (0.5%) of C-addition drastically reduced the CCS of the samples. A concomitant increase is observed thereafter for the third (1.0%) and fourth (2.0%) slabs might be due to the incorporation of hard (dry) solid agglomerates in the matrix. However, the ingress of moisture associated with the last slab (4.0%) hinders the effect of coprecipitated hard solids in the castable matrix showing a contemptible drop in CCS value. Therefore, it was somewhat difficult to compare these G and C precursors judiciously with preformed spinels, the latter being frequently applied to castables in much higher quantities [15,55–57] retaining their excellence.

Considering all these aspects, a newer batch of castable [Table 3] was formulated. In this respect, 8.0 wt.% of previous precursors (in a modified form) was incorporated separately in that batch, and their performances were compared with the same batch prepared with 8.0 wt.% of preformed spinel [Table 4] additive. As described in Section 2, the G and C precursors were optimally ground and calcined to produce the modified in situ additives with their characteristics shown in Table 2(b). Recently, the mechanochemical synthesis [45,46] of ceramic materials have been appreciated by many researchers. It has already been tried for $MgAl_2O_4$ system too [58]. It is suggested that the grinding of dry gels (G and C) before calcination assisted the homogeneization and activation of gel to evolve the spinel phase completely at lower temperature than observed before in the unground gels [22,24]. This is confirmed by Fig. 3(a), the XRD pattern at 600 °C of the ground G type gel, which strongly infers the evolution of nanocrystallites of spinels by the broadened nature of the prominent peaks [37,59]. This kind of refinement of structure and retention of nanocrystallinity might have been possible due to the mechanochemical amorphization of the dried precursor gel. However, Table 2(b) shows that the coprecipitated precursor could not reveal any remarkable development and showed

Table 6
Hot modulus of rupture (at 1400 °C) of castables

Sample	HMOR (kg/cm^2)
B	65
PN	128
GN	120
CN	75

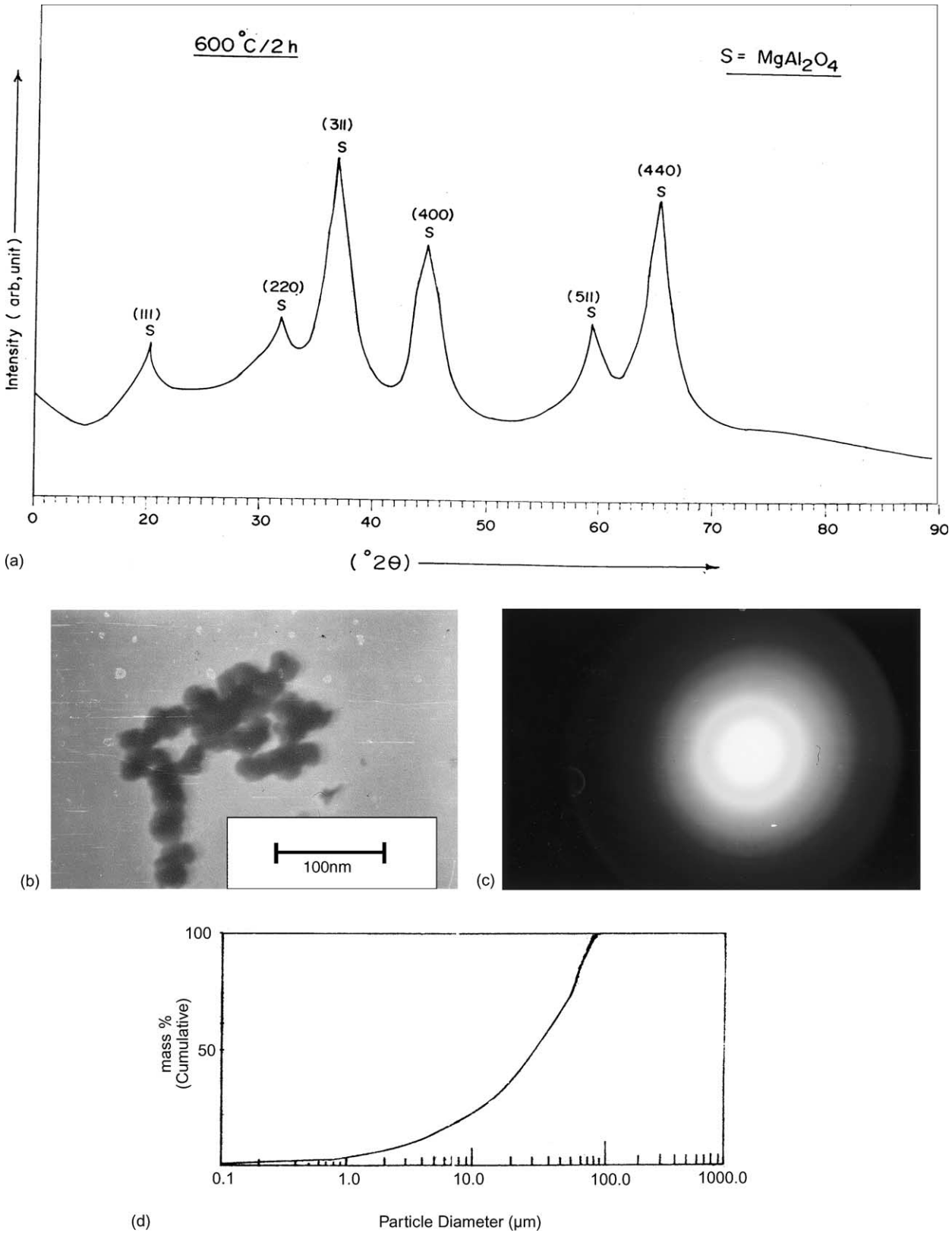

Fig. 3. (a) XRD pattern of ground G type gel after calcination at 600 °C/2h; (b) TEM micrograph; (c) SAED photograph of the modified G additive and (d) particle size distribution curve of modified in situ (G type) additive.

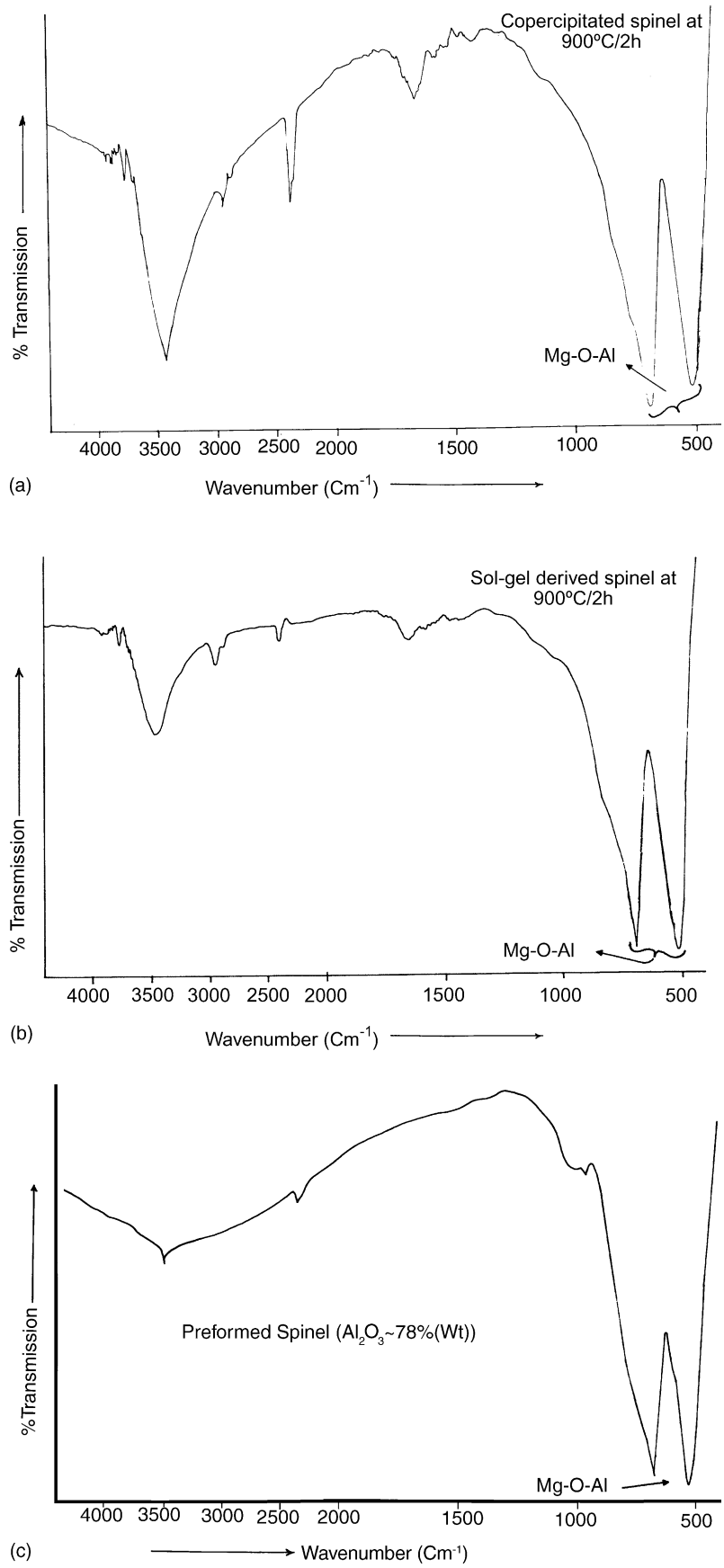

Fig. 4. (a) IR pattern of modified C type spinel additive; (b) IR pattern of modified G type spinel additive and (c) IR pattern of P type preformed spinel additive.

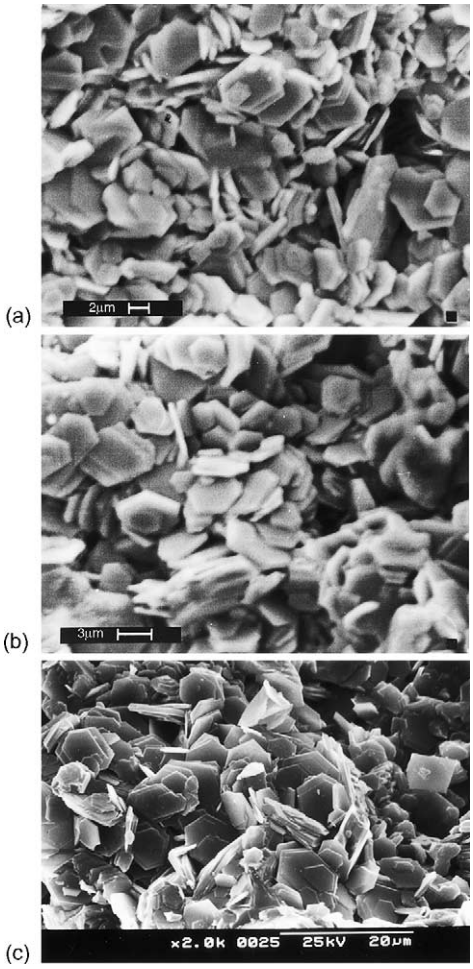

Fig. 5. SEM micrographs of (a) GN; (b) CN and (c) PN type castables (fired at 1600 °C/2 h).

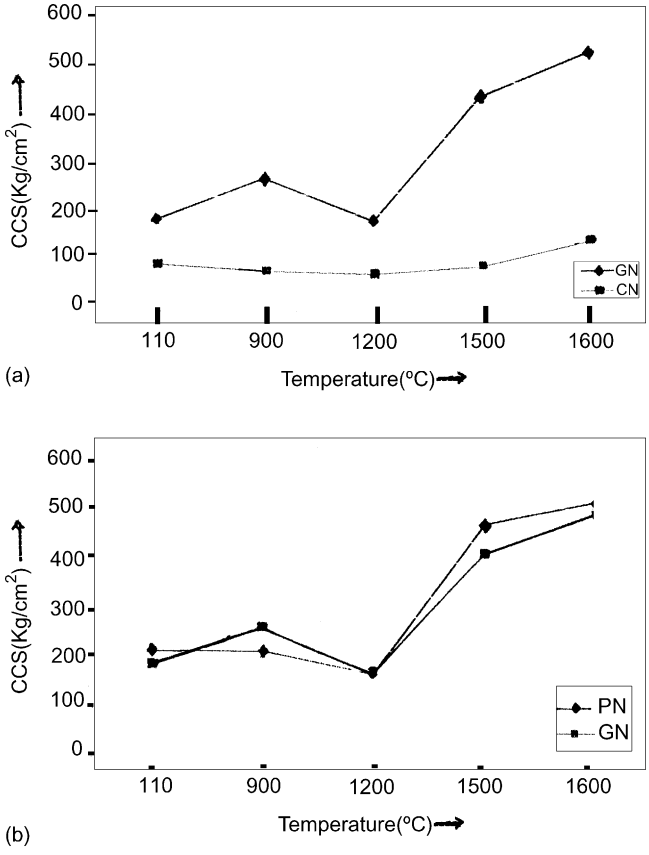

Fig. 6. Comparison of change in CCS property with temperature between different castables (a) GN and CN types; (b) GN and PN types.

spinel evolution at till higher temperature (1000 °C) with much larger crystallites as measured by Scherrer's formula [60]. The optimum calcination of ground gels at 900 °C was done to generate reactive sinterable spinel as suggested by Bratton [47] by balancing the tradeoff between surface area and relative density. It may be suggested that some part of the free energy change (during calcination) that has driven the decomposition had created an additional surface free energy. Moreover, to propagate the decomposition reaction at a faster rate during calcination, the material has been subdivided into small particles to minimize the diffusion distances. The grinding operation after calcination must have also been facilitated by the topotactic orientation relationship and large molar volume difference between the hydrated parent salt and calcined oxide; this has possibly created a high degree of coherency strain and cracks associated with the particles [61]. The post-calcination grinding additionally helped the particles to get associated with some stored energy [62] having activated surfaces. Lastly, the residual hydroxyl groups present after calcination in spinel additives (as shown afterwards) provided further convenience during communition to result in reactive additives in an energy efficient way. The friable G additive with finer pores was found to be easy-to-grind and soft;but the C additive was harder [58,63] might be due to uncontrolled agglomeration of the precursor particles. Another salient feature of the G additive was that it maintained its nanofineness as substantiated by Fig. 3(b) and (c). The TEM and SAED photographs clearly corroborate the close approach of this modified additive towards nanocrystallinity [35]. It possibly adds a benefit in castable property to retain nanostructuralisation in the matrix as discussed later. The precision of sol–gel route is also confirmed by Table 2(b) from the chemical analysis of the corresponding spinel composition, whereas the deviation is confirmed by the composition of coprecipitated material. The presence of nanoparticles in the modified G additive is also clear from the particle size distribution curve [Fig. 3(d)], whose lower end goes on decreasing up to almost 100 nm. As such it might be considered as the reactive matrix constituent of the new castable. The particles lying below 75 micron (−200 mesh) can be generally categorized as the matrix part of the castable [17,48]. It is interesting to note that such cost effective additive can be easily prepared in laboratory at relatively mild condition, indicating a possibility of energy and time saving without violating the precautions imposed for pollution abatement. However, the

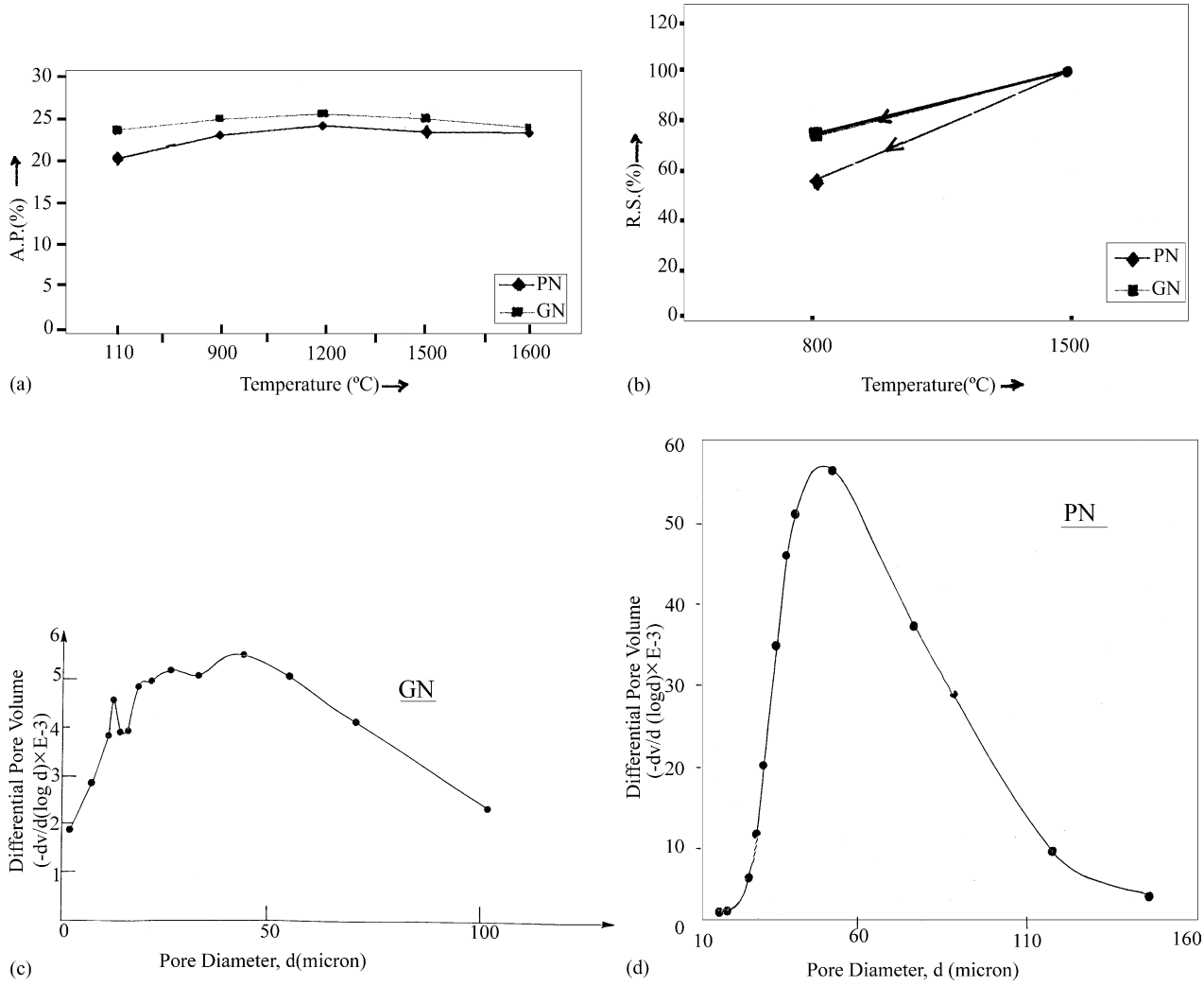

Fig. 7. (a) Comparison of change in AP values with temperature between GN and PN type castables; (b) variation in %RS values between GN and PN type castables; (c) comparison of pore size distribution patterns (in terms of differential pore volume vs. pore diameter) between GN and PN type castables.

preformed spinel (Table 4) usually is prepared in industry after a series of processing stages [16] and lastly by exhaustive vibrogrinding and milling operations with a possible escalation of cost and contamination constraints. It is known that conventional dry milling methods are energy intensive consuming around 15% of energy supplied for size reduction [61]. Wet milling, although is advantageous than dry, introduces inhomogeneities like binder, surfactant or sintering aids and needs further modification. Nevertheless, these modified additives were ground easily by agate in laboratory with no significant consumption of time and skill.

Table 2(b) further shows that the specific gravity of modified C additive is too low than G additive. It may be due to a lot of water associated in the structure of poorly dispersed hydrated spinel prepared by coprecipitation with a coarser scale of mixing. This is supported by the IR patterns [Fig. 4] of C and G additives which show that the broad band at around 3400 cm^{-1} for (OH) groups is more developed in C. It also possesses some entrapped (OH) and entangled amine groups in its calcined state as revealed by the peaks, respectively, at 1630 cm^{-1} (bending) and 1410 cm^{-1} might be due to uncontrolled precipitation. The peak for (OH) stretching at 3450 cm^{-1} in G is considerably less intense [64]. However, the peaks for Mg–O–Al linkage (inferring the spinel formation) ascribed within 525–690 cm^{-1} [65] are quite prominent in both the two additives like the preformed spinel (P) fine [Fig. 4(c)]. The excessive volatiles present in C additive might have liberated at further higher temperatures to create flaws in the castable matrix to result in substantial volume stress. The DTG pattern of coprecipitated spinel [24] done before also supported this kind of extended pyrolysis to release enormous amount of volatiles till 1000 °C. These excessive residual groups may also cause relatively less specific gravity of C as compared to the G additive [66]. The delay of complete spinel evolution in C possibly caused a lack of densification and poor sinterability of the resulting powder as mentioned later. Oppositely, the onset of spinellisation in G at lower temperature with less amount of residual OH– groups present in its structure resulted in higher specific gravity of the same. As the

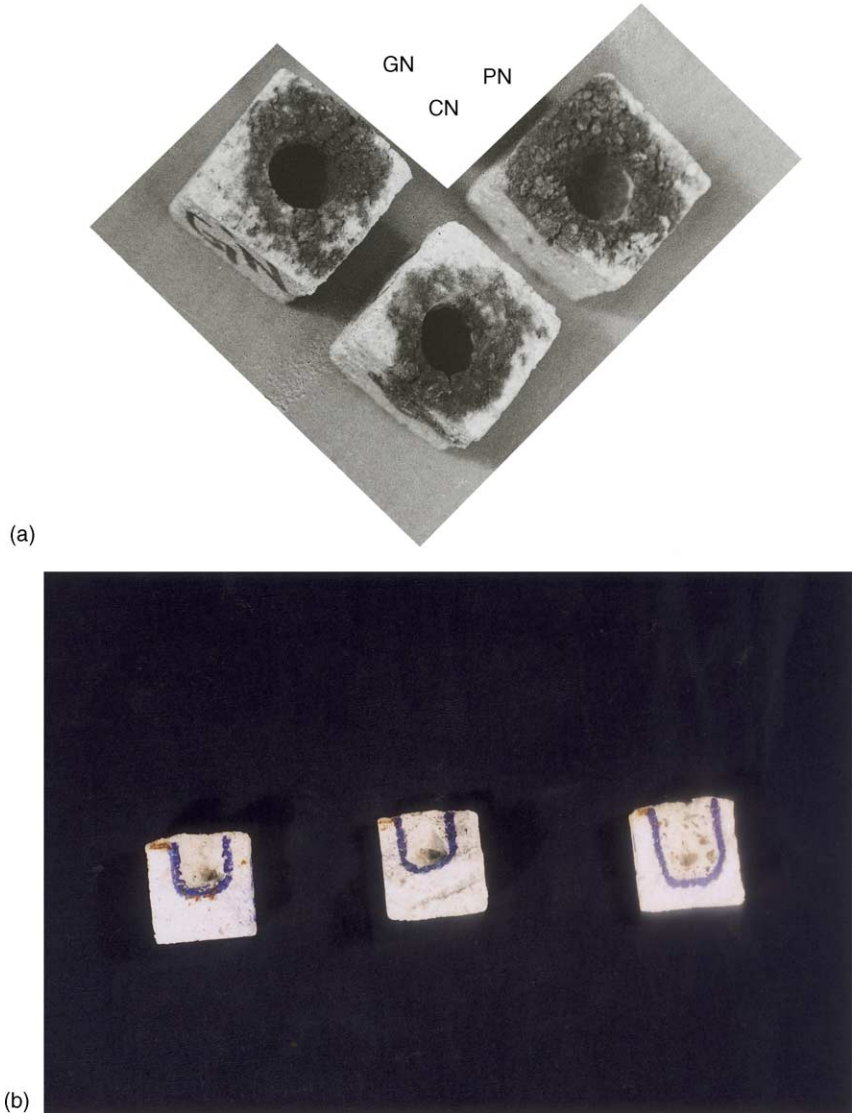

Fig. 8. (a) Effect of slag corrosion (by converter slag) in GN, CN and PN type castables and (b) cut section photograph of corroded castables (from LHS, GN, PN and CN type).

spinellisation started earlier from the molecularly mixed ingredients of G, possibly the densification of this material started earlier, and consequently, the improvement in specific gravity was much pronounced.

Fig. 5(a)–(c) shows the micrographs of, respectively, GN, CN and PN type castables after heat treatment at 1600 °C. They show the morphological similarity with enough of hexagonal CA_6 phases generated in all of them. These net like phases interconnect the corundum and spinel grains to improve the performance of such castables [67,68]. Reduction of microsilica possibly helped to raise the service temperature without any deformation of these castables. In spite of the morphological similarity, the properties of GN, CN and PN showed considerable difference as revealed from Figs. 6 and 7. The CCS value of GN was remarkably higher than CN and almost comparable to PN. Hokazono et al. [36] described the poor sinterability of spinel prepared via coprecipitation by nitrate precursors. In our work, also the poor density of the same was originated possibly due to less effectively mixed nitrates present in the precursor. As a consequence the bimodal distribution of particles [24,27] was found, that might have hindered the densification and delayed the spinel evolution in the modified form. This in turn deteriorated the properties of CN might be by some abnormal growth of grains. A lot of cracks generated by the volatiles released from the additive also caused a serious limitation in terms of AP and CCS of castable. However, the G additive with a precise control over its stoichiometry and due to the presence of reactive nanocrystalline spinels in its structure, might have easily formed the CMAS (MgO) phase [17,67] in castable and undue volume expansion has been reduced. The CCS of GN is better than PN below 900 °C for this desirable CMAS phase with an interwoven morphology to hold the grains. Nevertheless, the CCS after 900 °C is

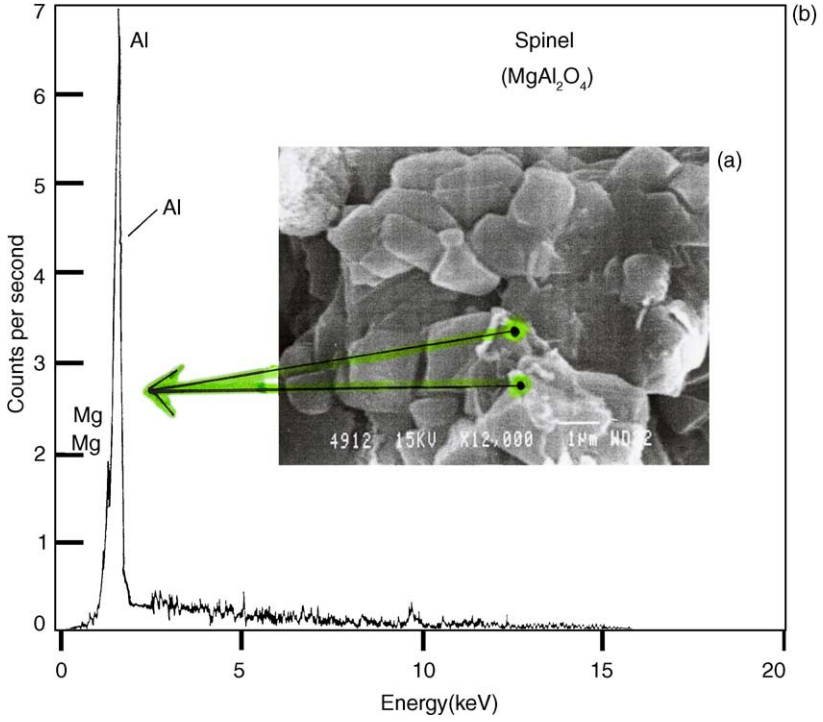

Fig. 9. (a) Micrograph of GN type castable (1600 °C/2 h) and (b) EDS trace of spinel phase.

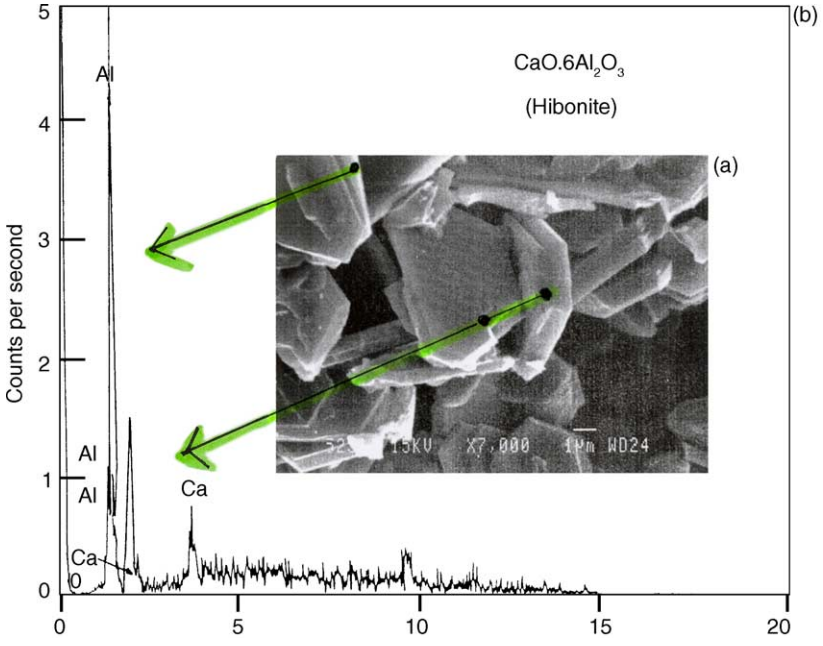

Fig. 10. (a) Micrograph of the fractured surface of GN type castable (1600 °C/2 h) and (b) EDS pattern of hibonite phase.

better in PN, because the true specific gravity of G additive is almost 17% less than the presintered densified spinel [Table 4]. Moreover, as the fineness of G was below 75 μm and that of P was below 45, thus the particle size effect also contributes a role [48,57] towards the strength values of castables. The limit of fineness was optimized to below 75 μm in G not to allow the chance of particle reaggregation on prolonged crushing [61]. The porosity of GN castable is poor in comparison to PN might be due to the remnant OH– groups present in the additive as corroborated before by IR pattern. However, this little increase in porosity may be sacrificed if those pores can be utilized to upgrade the %RS of GN in comparison with PN. Fig. 7(b) shows the improved spalling resistance of GN possibly due to the distributed micropores generated in castable by the residual OH groups present in the G-type modified spinel additive; however, the

P type additive lacked these (OH) groups as observed in the IR patterns. Therefore, retention of some hydroxyl groups in optimally calcined additive is necessary to create such microvents and cracks which might hinder the extension of flaws during thermal shock [53]. Fig. 7(c) supports the presence of a wider distribution of well scattered micropores (i.e. the crack-stoppers) in GN while that of PN is narrower with larger pores although its porosity is less. The improved performance and need of low density spinel-bonded castable have been the area of interest of some recent refractory scientists [69]. The G type modified additive, in this regard, may be considered beneficial because of its additional alliance with the nano-hypothesis.

Table 5 is the composition of converter slag used to evaluate the corrosion resistance of GN, CN and PN castables. Fig. 8(a) and (b) show that the properties of sol–gel based modified spinel-alumina castables are comparable to the preformed one as regards resistance to penetration and erosion. It is suggested that reactive spinel fines [56] entrap MnO, FeO, etc. from slag inside the voids of its structure to form complex spinel solid solutions. Consequently, the slag composition becomes rich in silica and could not penetrate into castable. It may further be suggested that the effectively dispersed nanocrystalline spinel interfaces present in GN castable presumably render a passive corrosion effect [4], with the advantage of finer pores and vents that restrict the slag penetration in castables. The depth of slag intrusion and wetting at aggressive condition is quite clear from the cross-sectional view (Fig. 8(b)) of the corroded specimens which again advocates the better performance of GN type castable than CN.

The origin of aggreable performance of GN type castable (substantiated with the nano-hypothesis) becomes more tangible from the other SEM and EDS (Fig. 9) figures of the corresponding fired material. It reveals that some nanofine spinel domains have been generated in matrix which are directly bonded with corundum and hibonite grains. This kind of modification of matrix by the self-assemblage of spinel crystallites is possible because of the effectiveness of sol–gel (G) additive. Although the microstructures having an average phase or grain size of the order of 10^{-9} mm are classified as nanoparticles, but in a wider meaning of the terminology [70] any region containing clusters or grains or layers up to 100 nm are considered to be as the nanostructured materials. Fig. 9(b) shows the spinel crystallites with nearly nanoscale dimensions are embedded in the matrix. The retention of such nanostructured phases after sintering is the additional benefit of the flexible sol–gel route which enables tuning the pore size, surface area, composition and density of the additive. The composition of those particles was found to be alumina-rich spinel. It may be suggested that this reactive sol–gel spinel took up some matrix alumina to form non-stoichiometric nanoclusters of spinel to generate some tiny microflaw in the respective castable. These flaws again upgraded the %RS of GN than PN by crack closure mechanism as per Hasselman's criterion [53].

The profilic existence of platy, hexagonal, cardlike crystals of CA_6 interlocked firmly with corundum and spinel grains in GN is prominent from Fig. 10. They occupied the space between medium and large sized grains and formed necks and bridges as found in the SEM of the fractured surface. It improved the HMOR of GN castable as observed from Table 6. This CA_6 phase confers an excellent three-dimensional linkage between aggregate and matrix [15,18,67,68]. This kind of connectivity possibly is not so extensive in CN might be due to the abnormal spinel grown in the corresponding matrix. However, the hot strength of PN was the best among all for which it is popularly used by the castable manufacturers with its very fine (below 45 μm) particles. It may also be noted that the hot strength observed for spinel-free castable (code B, Table 6) has been increased a lot possibly due to the elimination of low melting C–A–S phase in this second phase of investigation. For the same reason, the CCS and AP values of PN and GN castables were significantly poor than B sample due possibly to the absence of liquid phase sintering assisted by that C–A–S phase as observed before [26–29].

4. Conclusions

1. Spinel-alumina refractory castables can be conveniently fabricated by hydrated magnesium aluminate gels prepared via sol–gel and coprecipitation methods. The shortcoming of 4.0 wt.% of hydrated spinel bonded castables, e.g. their uncontrolled volume expansion, excessive porosity and poor green strength can be overcome by partly calcining and incorporating the ground powders (−75 μm, 8.0 wt.%) as modified in situ additives in castables.
2. Of those two, the nanocrystalline sol–gel additive holds a better prospect for reducing excess energy, time and cost required to produce the similar type castable by preformed spinels. The properties of preformed spinel bonded castables are better than sol–gel especially in terms of AP and the performance of agglomerated coprecipitate additive is the poorest among all. The thermal shock resistance of the castables bonded with sol–gel additive is exceedingly well, while their CCS and slag resistance properties are comparable to the preformed one.
3. Microfine silica content in both performed and in situ type spinel-alumina castables must be kept below a certain limit to improve the service temperature and HMOR property.

References

[1] J.H. Chesters, Refractories for Iron and Steel Making, The Metals Society, London, 1974.
[2] N. Moritama, Recent progress of steel making technology and expectation for refractories, Taikabutsu Overseas 6 (1986) 18–36.

[3] V. Kudrin, Steel Making, MIR Publishers, Moscow, 1985.
[4] W.E. Lee, R.E. Moore, Evolution of in situ refractories in the 20th century, J. Am. Ceram. Soc. 81 (1998) 1385–1410.
[5] A.R. Studart, R.G. Pileggi, W. Zhong, V.C. Pandolfelli, Processing of zero cement self flow high alumina refractory castable by matrix rheological control, Am. Ceram. Soc. Bull. 77 (1998) 60–66.
[6] S. Banerjee, Recent development in monolithic refractories, Am. Ceram. Soc. Bull. 77 (10) (1998) 59–63.
[7] G. Oprea, T. Troczynski, F. Esanu, in: Proceedings of the UNITECR on Rheology Studies on Binding Systems for Self Flow Refractory Castables, New Orleans, USA, 1997, pp. 613.
[8] H. Nishio, in: Proceedings of the UNITECR on Steelmaking Refractory Trends in Japan, Osaka, 2003, pp. 2–3.
[9] J. Mori, N. Watanabe, M. Yoshimura, Y. Oguchi, T. Kawakami, A. Matsuo, Material design of monolithic refractory for steel ladle, Am. Ceram. Soc. Bull. 69 (1990) 1172–1176.
[10] H. Kato, T. Takahashi, T. Kondo, Y. Ogura, Application of alumina-spinel castable refractory in ladle bottoms, Taikabutsu Overseas 16 (1996) 22–27.
[11] J. Madias, R.E. Caligaris, L. Zamboni, Post mortem study of alumina-spinel castables of an electric arc furnace roof, Interceram 49 (2000) 348–351.
[12] E. Ryshkewitch, Oxide Ceramics, Academic Press, New York, September 1960, pp. 257–274.
[13] Y.M. Chiang, D.P. Birnie, W.D. Kingery, Physical Ceramics: Principles for Ceramic Science and Engineering, Wiley, New York, 1997.
[14] C.F. Chan, Y.C. Ko, A study of commercial magnesia–alumina spinels for alumina-spinel castables, Interceram 47 (1998) 374–378.
[15] M.W. Vance, G.W. Kriechbaum, R.A. Henrichsen, G. Maczura, K.J. Moody, S. Munding, Influence of spinel additives on high-alumina/spinel castables, Am. Ceram. Soc. Bull. 73 (1994) 70–74.
[16] R.M. Evans, Magnesia–alumina-spinel, Am. Ceram. Soc. Bull. 72 (1993) 59–63.
[17] M. Fuhrer, A. Hey, W.E. Lee, Microstructural evolution in self-forming spinel/calcium aluminate bonded castable refractories, J. Eur. Ceram. Soc. 18 (1998) 813–820.
[18] Y.C. Ko, J.T. Lay, Thermal expansion characteristics of alumina–magnesia and alumina-spinel castables in the temperature range of 800–1650 °C, J. Am. Ceram. Soc. 83 (2000) 2872–2874.
[19] K.H. Hwang, K.D. Oh, R.C. Bradt, in: Proceedings of the UNITECR on In situ Spinel Bond Formation (Expansion/Contraction) During Firing, New Orleans, 1997, pp. 1575.
[20] K.G. Aghari, J.H. Sharp, W.E. Lee, Hydration of refractory oxides in castable bond systems-1 alumina, magnesia and alumina–magnesia mixtures, J. Eur. Ceram. Soc. 22 (4) (2002) 495–503.
[21] P. Lauzon, J. Rigby, C. Oprea, T. Troczynski, G. Oprea, in: Proceedings of the UNITECR on Hydration Studies on Magnesia-containing Refractories, Osaka, 2003, pp. 54–57.
[22] S. Mukhopadhyay, S. Ghosh, M.K. Mahapatra, M. Majumdar, P. Barick, S. Gupta, S. Chakraborty, Easy-to-use mullite and spinel sols as bonding agents in a high alumina based ultra low cement castable, Ceram. Int. 28 (7) (2002) 719–729.
[23] S. Ghosh, R. Majumdar, B.K. Sinhamahapatra, R.N. Nandy, M. Mukherjee, S. Mukhopadhyay, Microstructures of refractory castables prepared with sol–gel additives, Ceram. Int. 29 (6) (2003) 671–677.
[24] S. Mukhopadhyay, S. Sen, T. Maiti, M. Mukherjee, R.N. Nandy, B.K. Sinhamahapatra, In situ spinel spinel bonded refractory castable in relation to coprecipitation and sol–gel derived spinel forming agents, Ceram. Int. 29 (8) (2003) 857–868.
[25] D. DasPoddar, S. Mukhopadhyay, Spinel bonded basic castables in relation to spinel forming agents, Interceram 51 (4) (2002) 282–287.
[26] S. Mukhopadhyay, P.K. DasPoddar, Effect of preformed and in situ spinels on microstructure and properties of a low cement castable, Ceram. Int. 30 (3) (2004) 369–380.
[27] S. Mukhopadhyay, I. Chatterjee, R. Mukherjee, S.K. Nath, S. Sarkar, S. Mondal, S. Bhowmik, Prereacted and coprecipitated spinels as additives in a low moisture castable. Part 1, Ind. Ceram. 23 (3) (2003) 198–204.
[28] S. Mukhopadhyay, P.K. DasPoddar, Presintered and coprecipitated spinels as additives in a low moisture castable, part 2, Ind. Ceram. 24(1) (2004) 29–34.
[29] S. Mukhopadhyay, P.K. DasPoddar, Effect of preformed and in situ spinels on microstructure and properties of a low cement refractory castable, part 2, Ind. Ceram. 24 (2) (2004) 199–205.
[30] S. Mukhopadhyay, P.K. DasPoddar, G. Banerjee, in: Proceedings of the UNITECR on Influence of Prereacted and Self-reacting Spinels on the Characteristics of High Alumina Castable, 2003, pp. 158–161.
[31] J.C. Debsikdar, Preparation of transparent non-crystalline stoichiometric magnesium aluminate gel monolith by the sol–gel process, J. Mater. Sci. 20 (1985) 4454.
[32] J.K. Popovic, N. Miljevic, S. Zec, Spinel formation from coprecipitated gel, Ceram. Int. 17 (1991) 49–52.
[33] G. Gusmano, P. Nunziante, E. Traversa, G. Chiozzini, The mechanism of $MgAl_2O_4$ spinel formation from the thermal decomposition of coprecipitated hydroxides, J. Eur. Ceram. Soc. 7 (1991) 31–39.
[34] V. Montouillout, D. Massiot, A. Douy, J.P. Coutures, Characterisation of $MgAl_2O_4$ precursor powders prepared by aqueous route, J. Am. Ceram. Soc. 82 (1999) 3299–3304.
[35] R.K. Pati, P. Pramanik, Low temperature chemical synthesis of nanocrystalline $MgAl_2O_4$ spinel powder, J. Am. Ceram. Soc. 83 (2000) 1822–1824.
[36] S. Hokazono, K. Manako, A. Kato, The sintering behaviour of spinel powders produced by a homogeneous precipitation technique, Br. Ceram. Trans. J. 91 (1992) 77–79.
[37] J.F. Pasquier, S. Komarneni, R. Roy, Synthesis of $MgAl_2O_4$ spinel: seeding effects on formation temperature, J. Mater. Sci. 26 (1991) 3797–3802.
[38] A.R. Studart, F.S. Ortega, M. Innocentini, MDM, V.C. Pandolfelli, Gelcasting high alumina refractory castables, Am. Ceram. Soc. Bull. 81 (2002) 42.
[39] P. Janeway, Nanotechnology—it's more than size, Am. Ceram. Soc. Bull. 82 (4) (2003) 31–38.
[40] S. Tamura, T. Ochiai, T. Kanai, H. Nakamura, Nano-tech refractories 2, in: Proceedings of the UNITECR on The Application of the Nanostructural Matrix to MgO–C Bricks, 19–22 October, Osaka, Japan, 2003, pp. 521–524.
[41] Ibid, Nano-tech refractories-1, The Development of the Nanostructural Matrix, pp. 517–520.
[42] A.R. Studart, W. Zhong, V.C. Pandolfelli, Rheological design of zero-cement self flow castables, Am. Ceram. Soc. Bull. 78 (5) (1999) 65–72.
[43] P. Bonadia, A.R. Studart, R.G. Pileggi, V.C. Pandolfelli, Applying MPT principle to high alumina castables, Am. Ceram. Soc. Bull. 78 (3) (1999) 57–60.
[44] H. Bhattacharya, B.N. Samaddar, Formation of non-stoichiometric spinel on heating hydrous magnesium aluminate, J. Am. Ceram. Soc. 61 (5–6) (1978) 279–280.
[45] J. Temuujin, K. Okada, J.K.D. Mackenzie, Formation of mullite from mechanochemically activated oxides and hydroxides, J. Eur. Ceram. Soc. 18 (1998) 831–835.
[46] S. Kawai, M. Yoshida, G. Hashizume, Preparation of mullite from kaolin by dry grinding, J. Ceram. Soc. Jpn. 98 (1990) 669–674.
[47] R.J. Bratton, Characterisation and sintering of reactive $MgAl_2O_4$ spinel, Am. Ceram. Soc. Bull. 48 (11) (1999) 1069–1075.
[48] Y.C. Ko, C.F. Chan, Effect of spinel content on hot stregth of alumina-spinel castables in the temperature range 1500 °C, J. Eur. Ceram. Soc. 19 (1999) 2633–2639.
[49] C.F. Chan, F.J. Huang, Y.C. Ko, Refractoriness under load of alumina-spinel castables, Interceram 46 (1997) 86–89.
[50] Y.C. Ko, in: Proceedings of the UNITECR on Influence of Microsilica Addition on the Properties of Alumina-Spinel Castables, Berlin, Germany, 1999, pp. 22–25.

[51] M. Ramakrishna Rao, Liquidus relations in the quaternary subsystem $CaAl_2O_4$–$CaAl_4O_7$–$Ca_2Al_2SiO_7$–$MgAl_2O_4$, J. Am. Ceram. Soc. 51 (1968) 50–54.
[52] ASTM specification, C 20-00 and C 133-94.
[53] D.P.H. Hasselman, Unified theory of thermal shock fracture initiation and crack propagation in brittle ceramics, J. Am. Ceram. Soc. 52 (1969) 600–604.
[54] K. Nihara, M. Kusunose, T. Nakayama, T. Sekino, Y. Hayashi, Process structure, property and applications of ceramic based nanocomposites with multifunctionality, in: Proceedings of the 67th Annual Session of Indian Ceramic Society, 9–11 January, Chennai, India, 2004.
[55] G. Maczura, M. Madono, G.W. Kriechbaum, B. Sewell, in: Proceedings of UNITECR on Low Moisture Regular Corundum/Spinel Castables with Superior Properties, Kyoto, Japan, 1995, pp. 179–186.
[56] P. Korgul, P.R. Wilson, W.E. Lee, Microstructural analysis of corroded alumina-spinel castable refractories, J. Eur. Ceram. Soc. 17 (1997) 77–84.
[57] Y.C. Ko, Influence of total fines content on the thermal shock damage resistance of alumina-spinel castables, Ceram. Int. 27 (2001) 501–507.
[58] G. Ye, T. Troczynski, G. Oprea, in: Proceedings of the UNITECR on Development of Reactive $MgAl_2O_4$ spinel powder, Osaka, Japan, 2003, pp. 168–171.
[59] C.C. Yong, J. Wang, Mechanical-activation-triggered gibbsite-to-boehmite transition and activation-derived alumina powders, J. Am. Ceram. Soc. 84 (6) (2001) 1225–1230.
[60] M.P. Klug, L.E. Alexander, X-ray Diffraction Procedure for Polycrystalline and Amorphous Materials, Wiley, New York, 1974.
[61] S.J. Schneider Jr., H.F. Lampman, N.D. Wheaton, Engineered Materials Handbook, vol. 4, Ceramics and Glasses, ASM International, The Materials Information Society, USA, 1991, pp. 75–78.
[62] M. Sathiyakumar, F.D. Gnanam, Synthesis of sol–gel derived alumina powder: effect of milling and calcination temperatures on sintering behaviour, Br. Ceram. Trans. J. 98 (1999) 87–92.
[63] J.G. Li, T. Ikegami, J.H. Lee, T. Mori, Y. Yajima, A wet-chemical process yielding reactive magnesium aluminate spinel powder, Ceram. Int. 27 (4) (2001) 481–489.
[64] Brian Smith, Infrared Spectral Interpretation: A Systematic Approach, CRC Press LLC, USA, 1999.
[65] M.P. O'Horo, A.L. Frisillo, W.B. White, Lattice vibrations of $MgAl_2O_4$ spinel, J. Phys. Chem. Solids 34 (1) (1973) 23–28.
[66] C.E. Scott, J.S. Reed, Analysis of Cl ions laundered from submicron zirconia powder, Am. Ceram. Soc. Bull. 57 (1978) 741–743.
[67] F. Simonin, C. Olagnon, S. Maximilien, G. Fantozzi, Thermomechanical behaviour of high alumina refractory castables with synthetic spinel additions, J. Am. Ceram. Soc. 83 (2000) 2481–2490.
[68] N.M. Khalil, M.F.M. Zawrah, Improvement of physico mechanical properties of self-forming MA spinel castables, Trans. Br. Ceram. 100 (2001) 110–114.
[69] R. Chen, P. He, N. Wang, J. Mon, F. Gan, in: Proceedings of UNITECR on Development of a Low Density Castable for Steel Ladle, Osaka, 2003, pp. 270–272.
[70] H.S. Nalwa (Ed.), Handbook of Nanostructured Materials and Nanotechnology, vol. 1, Academic Press, USA, 2000, pp. 216–388.